Electrochemical Interrogation of Kinetically-Controlled Dendritic DNA/PNA Assembly for Immobilization-Free and Enzyme-Free Nucleic Acids Sensing

Feng Xuan,[†] Tsz Wing Fan,[‡] and I-Ming Hsing*[,†,‡]

[†]Division of Biomedical Engineering and [‡]Department of Chemical and Biomolecular Engineering, The Hong Kong University of Science and Technology, Clear Water Bay, Kowloon, Hong Kong

ABSTRACT We present an immobilization-free and enzyme-free electrochemical nucleic acid sensing strategy, which uses kinetically controlled dendritic assembly of DNA and peptide nucleic acid (PNA). In the presence of a target sequence, ferrocene-labeled PNA probes (Fc-PNAs) and specially designed DNA strands are autonomously assembled into dendritic nanostructures through a cascade of toehold-mediated strand displacement reactions. The consumption of freely diffusible Fc-PNAs (neutrally charged), due to incorporation to DNA/PNA dendrimer, results in a significant electrochemical signal reduction of Fc on a negatively charged electrode from which the hyperbranched and negatively charged dendrimer of DNA/PNA would be electrostatically repelled. The cascade-like assembly process and large electrostatic affinity difference between Fc-PNAs and DNA/PNA dendrimer toward the sensing electrode offer a detection limit down to 100 fM and an inherently high specificity for detecting single nucleotide polymorphisms. The target-triggered mechanism was examined by PAGE analysis, and morphologies of the assembled dendrimers were verified by AFM imaging.

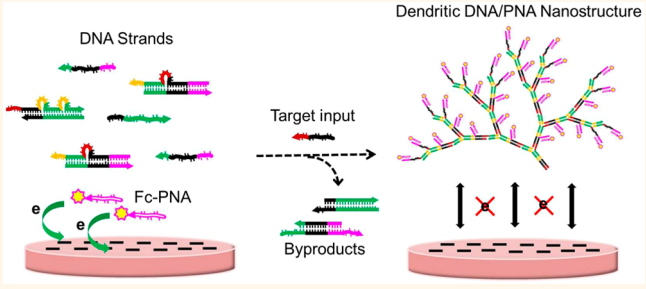

KEYWORDS: DNA/PNA dendrimer · kinetically controlled assembly · electrochemical detection · immobilization-free · enzyme-free

Electrochemical sensing methods for minute nucleic acid samples (e.g., DNA, microRNA) offer attractive opportunities for decentralized genetic testing which require portable, cost-effective, and low-power readout devices, and therefore have been intensively studied in the past decade.[1,2] Unlike the fluorescence-based optical nucleic acid sensing methods (NASMs) which can be easily operated in homogeneous solution,[3] most of the reported electrochemical NASMs are based on heterogeneous assay in which probe surface-immobilization is indispensable and probe-target interaction occurs at the interface between solution and electrode.[4−7] To achieve high sensitivity, the probe immobilization process usually demands laborious optimization of surface chemistry and coverage to maximize hybridization efficiency and meanwhile minimize nonspecific binding/adsorption. Even so, configurational freedom of the surface-immobilized probe is still restrained due to the steric hindrance effect of the electrode surface, resulting in reduced hybridization kinetics and specificity. Immobilization-free electrochemical NASMs[8] which employ solution-phase probes and bare detecting electrodes can potentially overcome the drawbacks in traditional immobilization-required electrochemical NASMs. However, the electrochemical signal transduction of immobilization-free electrochemical NASMs relies on the diffusion of electro-active molecules from the solution phase to the surface of the electrode. This diffusion-controlled nature results in a lower sensitivity compared to the immobilization-required approaches in which the electro-active molecules are

* Address correspondence to kehsing@ust.hk.

Received for review December 20, 2014 and accepted April 14, 2015.

Published online April 14, 2015
10.1021/nn507282f

attached or adsorbed on the electrode surface. Although efforts are made to improve the sensitivity of the immobilization-free electrochemical NASMs by incorporating enzyme-assisted signal amplification strategies,[9−12] the detection sensitivities achieved are still not competitive to fulfill the requirements of practical applications. Meanwhile, enzyme-assisted signal amplification strategies easily bring issues such as nonspecific enzyme adsorption on bare electrode surface, strict reaction conditions, and possible false-positives of enzymatic amplification process. Therefore, upgrading the detection sensitivity of immobilization-free electrochemical NASMs with enzyme-free strategies would be a desirable option, yet the challenge is how to exponentially amplify the electrochemical signal difference between sensing species without the assistance of enzyme.

As a vital part of recent advances in DNA nanotechnology,[13−16] kinetically controlled DNA self-assembly has emerged as a rapidly developing field.[15] Through rational design strategy of sequences, a single DNA strand is able to trigger a cascade of toehold mediated strand displacement (TMSD) reactions[17] between metastable monomers, assembling them into perceived target structures. The hybridization chain reaction (HCR) introduced by Pierce and Dirks in 2004 is one of the well-known strategies[18] and has been widely applied in biosensing as a reliable enzyme-free signal amplification approach.[19−25] In HCR, the cross-opening of two DNA hairpins triggered by a primary recognition event leads to autonomous formation of polymeric nanowires and enables linear detection signal amplification. In addition to one-dimensional self-assembly of HCR, nonlinear versions of HCR that result in formation of higher dimensional nanostructures are possible. Yin *et al*. demonstrated triggered self-assembly of multiarm DNA junctions and branched DNA dendrimers in their work on programming DNA self-assembly pathways.[26] LaBean *et al*. also reported a dendritic DNA self-assembly approach by designing two-loop structured hairpins.[27] These hairpin-mediated systems employ assembling monomers with specific secondary structures, making sequence design relatively complex and restrictive. Besides, improved DNA hairpin purification is needed in order to reduce the spontaneous initiation (system leakage). To overcome this, we have recently reported a hairpin-free system in which double-stranded DNA monomers could dendritically assemble into highly branched nanostructures upon detection of a target sequence, resulting in exponential growing kinetics with low system leakage.[28] This method adopts a simple sequence design strategy, and the modularity of its two-dimensional assembly process allows good flexibility for further functionality design.

Peptide nucleic acids (PNA) are DNA analogues in which the negatively charged sugar−phosphate backbone is replaced by a structurally homomorphous and uncharged polyamide backbone. The charge neutrality and high rigidity of its backbone offer superior thermal stability and hybridization kinetics of PNA/DNA binding.[29] In the present work, we engineer our dendritic assembly system to functionally "collect" PNA strands from the reaction mixture by taking the advantage of the superiority of PNA/DNA binding and achieve ultrasensitive and selective electrochemical DNA detection without employing a surface-immobilized probe or enzyme-assisted signal amplification. In the presence of a target sequence, self-assembly of DNA/PNA dendritic nanostructures could be rapidly initiated and grown in size. During this assembly process, a large amount of freely diffusible ferrocene-linked PNAs (Fc-PNAs) will be incorporated into the less-mobile DNA/PNA dendrimer, leading to amplified electrochemical signal reduction of Fc on a negatively charged electrode from which the assembled hyperbranched and negatively charged dendrimer of DNA/Fc-PNA would be electrostatically repelled.[30] This new approach employs a cascade-like self-assembling process plus a unique signal-transduction strategy taking advantage of differential electrostatic affinities of PNA and DNA/PNA dendrimer to a sensing electrode with negative charge, which results in electrochemical signal differentiation in an exponential manner and offers a detection limit down to 100 fM with excellent specificity.

RESULTS AND DISCUSSION

The schematic of the sensing strategy is illustrated in Figure 1. Components of which involve two double-stranded DNA probes, namely the sensing probe (SP) and PNA collector (PC); two single-stranded DNA, named assistant-1 (A1) and assistant-2 (A2); one Fc-PNA probe and a negatively charged indium tin oxide (ITO) electrode surface. SP and PC both possess protruding toehold domain[17] (5nt) and bulge loop domain (5nt+2nt) by annealing two partially complementary single-stranded DNA together. Complementarity relationships between different domains of SP, PC, A1, A2, and Fc-PNA were carefully exploited, and their sequences were specifically designed (Figure 1A). In the absence of target sequence, all the possible binding sites of these reagents are sequestered in either double-stranded form or bulge loops, kinetically impeding them from "reacting" with each other.[31] Under this circumstance, Fc-PNAs can freely access to the ITO electrode surface due to their neutral backbones, being electrochemically detectable (Figure 1B).

The cascade-like self-assembly process is triggered soon after the introduction of a target sequence (Figure 1C). This begins from the complementary binding between the target sequence and the toehold of SP, initiating the first TMSD reaction which displaces the black sequence domain to open the first loop. The

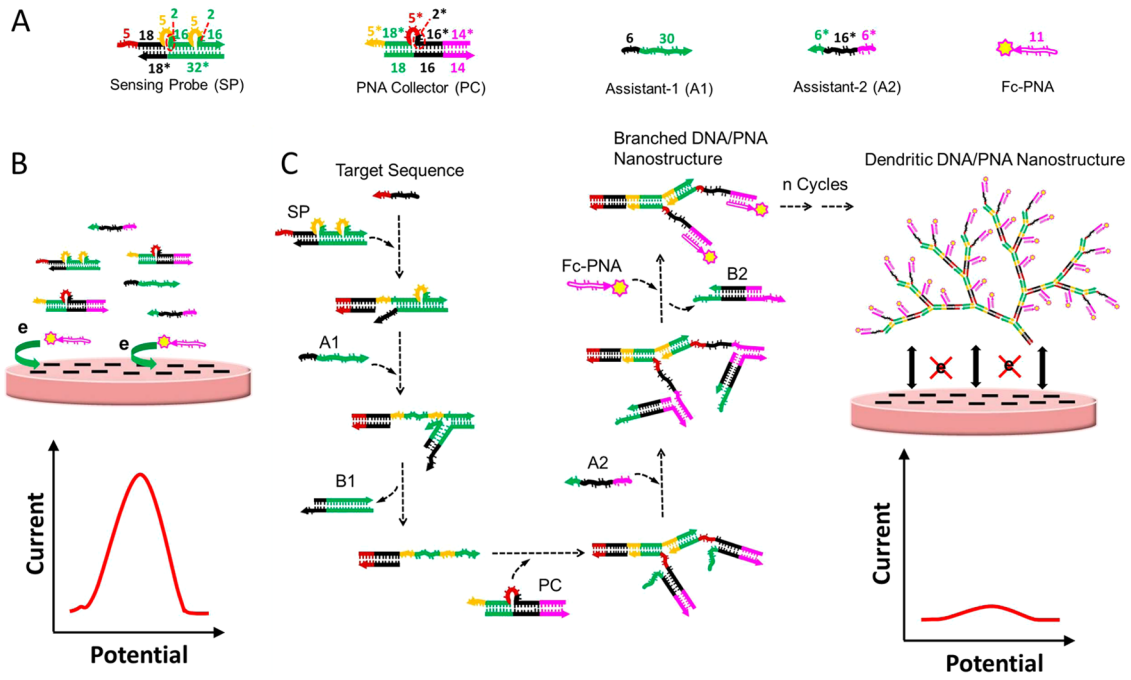

Figure 1. Electrochemical sensing mechanism and reaction pathway of the target-triggered assembly of dendritic DNA/PNA nanostructures. Lengths of different domains of designed reagents are indicated. DNA sequences drawn in the same color are either identical or complementary. For instance, 16* (black) is complementary to 16 (black).

opened loop allows the last six bases of the displaced strand form a new toehold to which A1 can hybridize. A1 then dissociates all but the last two base-pairs of the green domain by TMSD, opening the second loop. Displacement is completed by spontaneous dissociation of the remaining two base-pairs, releasing byproduct-1 (B1). The two opened sequences of SP can now bind to the toeholds of two PC, allowing the invasion of A2 after the loops of PC are opened through TMSD. Differently, A2 initiates a reversible TMSD that momentarily disassociates the first six base-pairs of the pink domain as "transient" toehold. Because of the faster hybridization kinetics and stronger binding strength between PNA and DNA,[29] Fc-PNA can bind to this momentarily exposed toehold and irreversibly disassociate the remainder but for the last three base-pairs of PC. After the spontaneous release of byproduct-2 (B2), a branched DNA/PNA nanostructure with two single-stranded target sequences is formed. These two target sequences are capable of initiating more rounds of similar TMSD reactions to "collect" more free Fc-PNAs in the solution, resulting in dendritic growth of the DNA/PNA nanostructure. The finally assembled DNA/PNA dendrimer, because of its hyperbranched structure and negatively charged DNA backbone, can hardly be in close proximity to the negatively charged ITO electrode surface. Therefore, a single target sequence converts massive freely diffusible Fc-PNAs to an indiffusible ensemble in the dendrimer, giving rise to an amplified reduction of the electrochemical signal (signal-off).

Cascade-like assembly reactions were performed in 1 × TAE buffer supplemented with 12.5 mM Mg^{2+} (pH = 8.0). SP and PC were prepared separately in a slow annealing process, where mixtures of the longer strand (4 μM) and the shorter strand (6 μM) were heated to 85 °C for 5 min and slowly (1 °C/min) cooled to room temperature. The excess shorter strands would make sure all the longer strands are protected in a designed form. The annealed SP and PC were first mixed with their corresponding assistants (8 μM) separately to remove the remaining shorter strands by preforming B1 and B2. The two resulting solutions were then mixed with Fc-PNA in a ratio of 1:2:2, giving final concentrations of 0.5 μM SP, 0.75 μM A1, 1 μM PC, 1.5 μM A2, and 1 μM Fc-PNA in the mixture. Finally, different amounts of target DNA were introduced.

Native polyacrylamide gel electrophoresis (PAGE) was used to verify the designed mechanism step by step. Fc-PNA in PAGE experiments was replaced by Cy5-labeled PNA (Cy5-PNA) with the same sequence, which made it possible to visualize PNA in the gel. SYBRGreen-stained DNA shows green color in the gel, while Cy5-PNA appears red. Therefore, any presence of DNA/Cy5-PNA hybrid structures would produce a yellow color. First, we demonstrate the catalytic formation of DNA/PNA hybrid structure between the designed PC and PNA probe. A short strand (named PC-Trigger) which possesses the same sequence with the repeated domain on SP was used to activate the "PNA collecting" function of PC (Figure 2A). Figure 2B shows the good stability between the designed PC and PNA probe when there are no A2 and PC-trigger. PC was challenged with 10 times the concentration of Cy5-PNA. After being incubated at room temperature over 5 h,

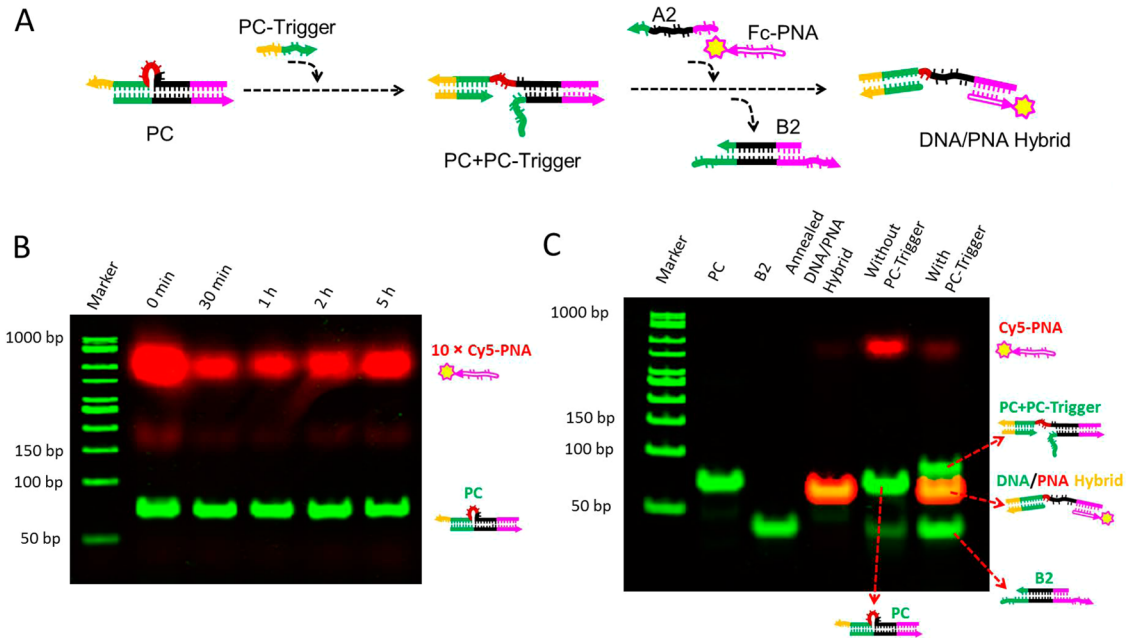

Figure 2. (A) Catalytic assembly pathway of the "PNA collecting" process of PC triggered by designed PC-trigger strand. (B) PAGE (8% gel) analysis of the stability between the designed PNA probe and PC. One μM PC was mixed with 10 μM Cy5-PNA and incubated at room temperature over 5 h. (C) PAGE (8% gel) analysis of the catalytic formation of DNA/PNA hybrid structure between PC and PNA probe. The final concentrations of PC, A2, Cy5-PNA, and PC-trigger in the reaction mixtures are 1 μM, 1.5 μM, 1 μM, and 1 μM, respectively. The samples were incubated at room temperature for 30 min. All images were taken at two different excitation/emission wavelengths and then overlaid.

there is still no sign of the binding event between PNA and PC (no yellow band shows). When PC, Cy5-PNA, and A2 were mixed under assembling conditions, as shown in the fifth lane of Figure 2C, the PC and PNA probes are still kinetically impeded from forming the DNA/PNA hybrid structure. The dim band with the fastest mobility indicates the small quantity of preformed B2. The addition of PC-trigger (the sixth lane of Figure 2C) causes an obvious change in the band shift of PC due to the complex formation of PC+PC-trigger. Meanwhile, the yellow band representing the DNA/PNA hybrid structure and large increase in B2 quantity are observed. These results indicate that the designed catalytic "PNA collecting" function of PC can be successfully implemented with the assistance of A2.

The whole kinetically controlled assembly process of DNA/PNA dendritic nanostructure was then demonstrated. As shown in Figure 3A, in the absence of target sequences, there is no sign of DNA/PNA hybrid, showing a good stability between the designed SP, A1, PC, A2, and PNA probe. The addition of a target shows the formation of DNA/PNA hybrid structures with a broad distribution and the average molecular weight is inversely related to the target concentration. Atomic force microscopy (AFM) imaging of the assembled products further confirmed the above PAGE data and reveals the expected dendritic morphology. In the absence of targets, Figure 3B only shows some tiny spots which represent the unassembled reagents and preformed byproducts, showing no sign of polymerization. In contrast, different sizes of dendritic structures

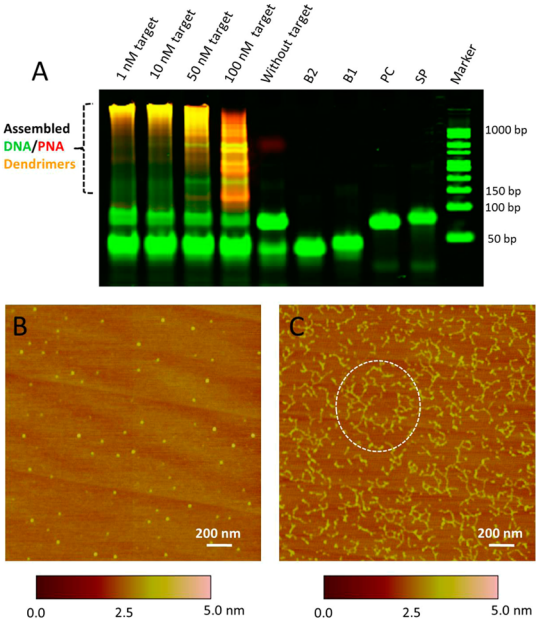

Figure 3. (A) PAGE (8 % gel) analysis demonstrated the kinetically controlled assembly mechanism of dendritic DNA/PNA nanostructures. Images taken at two different excitation/emission wavelengths were overlaid. (B, C) AFM images of the assembled products in the absence (B) and presence (C) of 10 nM target. All the samples were reacted at room temperature for 30 min.

are formed in the presence of the target sequence (Figure 3C). The observed dendritic assembly products evidently support the occurrence of cascade-like TMSD reactions as designed.

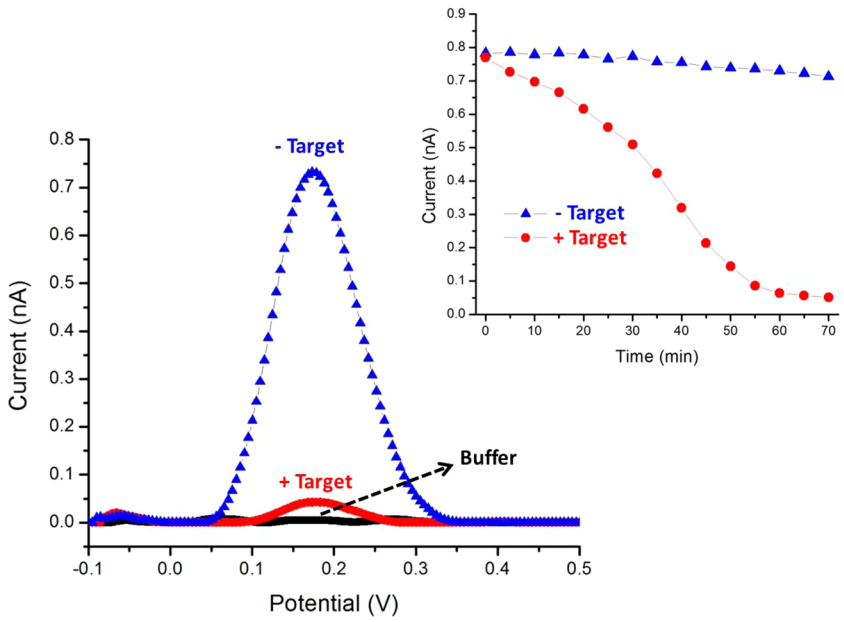

Figure 4. DPV scans of the assembled products in the absence (−) and presence (+) of 10 nM target, after being reacted at room temperature for 60 min. Inset: The sizes and morphologies of assembled polymers under certain trigger concentration are both highly polydispersed against incubation time in every 5 min.

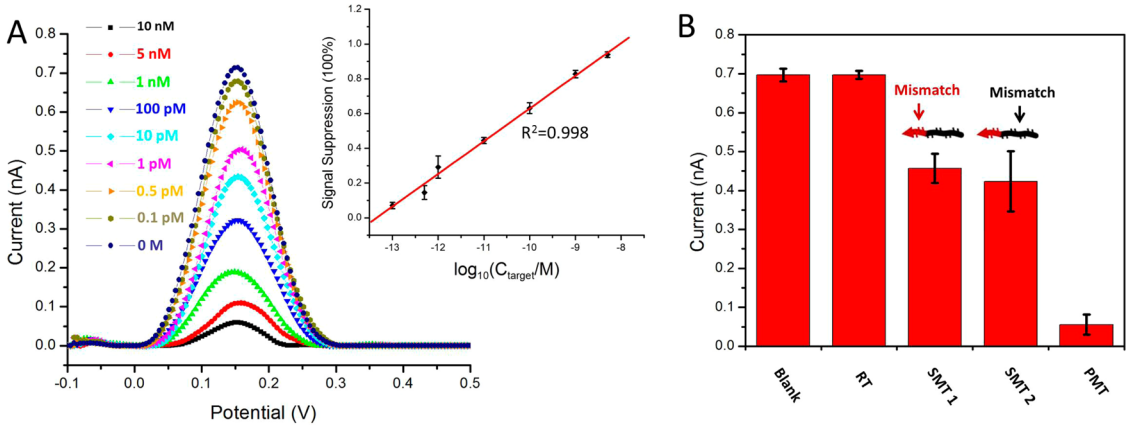

Figure 5. (A) DPV scans of the assembled products triggered by varying concentrations of target. Inset: Linear fit of the calculated peak current suppression percentage against the logarithm of target concentration. Signal suppression = $(I_0 - I_n)/(I_0 - I_{10\ nM})$, where I_n denotes the peak current of n M target and I_0 denotes the peak current of 0 M target. (B) Bar chart of the DPV responses of 0 nM target (blank), 10 nM random target (RT), two kinds of 10 nM single-base-mismatched targets (SMT1 and 2), and 10 nM perfectly matched target (PMT). All the samples were reacted at room temperature for 60 min. Mean values and standard deviations are obtained from three independent experiments.

Electrochemical measurements were further conducted on a fabricated microchip with conventional three-electrode system (Supporting Information, Figure S1) to characterize the accessibility difference between free Fc-PNA and assembled DNA/PNA dendrimer toward the negatively charged ITO electrode surface. It was found, as the differential pulse voltammetry (DPV) scanning results show in Figure 4, that the peak signal of Fc-PNA is remarkably reduced during the course of triggered dendrimer assembly, compared to that with no target input. The peak current becomes unnoticeable after 60 min of reaction time (inset of Figure 4), which supports well the signal-off mechanism as a result of the electrostatic repulsion and the size effect between the DNA/PNA dendrimer and the negatively charged electrode. On the other hand, accumulative reduction of peak current vividly indicates the ongoing scavenger of free Fc-PNAs during the dendrimer growth. This salient feature provides a competitive advantage of this new strategy on detection sensitivity. As shown in Figure 5A, 0.1 pM detection limit was readily achieved within 60 min. Above this limit, we observed a monotonic decrease in peak current intensity with increasing target concentration and the peak current suppression percentage showed a good linear correlation with the logarithm of target concentration in the range from 0.1 pM to 10 nM. The system is also highly specific. It is capable of distinguishing

between a perfectly matched target and a single-base-mismatched one with great signal difference, insensitive to the mismatch location in the toehold binding domain or not (Figure 5B). The high specificity, we believe, comes from the unrestrained configurational freedom of solution-phase probes combined with the TMSD reaction in which single-base mismatch would lead to significant kinetics change of both toehold binding and branch migration processes.[32]

CONCLUSION

To summarize, we have demonstrated a simple, rapid, immobilization-free, enzyme-free, ultrasensitive, and selective electrochemical nucleic acid sensing method based on a kinetically controlled assembly system in which specially designed DNA and Fc-PNA strands form DNA/Fc-PNA dendrimers only on detection of a target sequence. By growing to a hyperbranched structure with a negatively charged backbone, these dendrimers extinguish a electrochemical signal of the substantial assembled Fc-PNAs toward a negatively charged ITO electrode, providing amplified signal change to quantify the number of triggering targets. Different from all the reported electrochemical sensing methods, the achieved ultrahigh sensitivity and specificity require neither a sophisticatedly modified detecting electrode nor a susceptible assistant enzyme. This system functions at constant room temperature with inexpensive and handy instrumentation. Thus, it shows great potential to become a feasible approach for in situ rapid diagnosis of infectious disease out of a regular laboratory.

METHOD

Sequence Design. All the DNA oligonucleotides were purchased from Integrated DNA Technologies, Inc. (USA) and purified by PAGE. Fc-PNA and Cy5-PNA were purchased from Panagene (Korea). Predicted interactions of DNA strands were examined using Nupack.[33] The loop sequence on SP and PC was designed to be 2nt longer than the toehold. A1 was designed to be 2nt shorter when disassociating SP and Fc-PNA was designed to be 3nt shorter when disassociating PC. The purpose of these designs is to add 2nt or 3nt clamping segments at each end of SP and PC, which can prevent the possible interactions between these strands caused by "breathing" phenomenon at each end of ds structure.[26] Special emphasis of sequence design was placed on ensuring that A1, A2, and PNA possessed no significant secondary structure at room temperature, because strong secondary structure would greatly slow the rates of hybridization and branch migration.[34]

ITO Electrode Chip and Electrochemical Measurements. The fabrication of ITO-coated glass chip used for electrochemical measurement was done in the Nanoelectronics Fabrication Facility (NFF) of our University. The glass chip has one pair of platinum (Pt) pseudoreference and counter electrodes (thickness of 100 nm) as well as four working electrodes made of ITO (thickness of 100 nm), see the left panel of Supporting Information, Figure S1. The active surface area of each of the four ITO working electrodes is 7.85×10^{-3} cm^2. The potential of the Pt pseudoreference electrode in the 1 × TAE/Mg^{2+} buffer (1 × TAE buffer supplemented with 12.5 mM Mg^{2+}, pH = 8.0) was determined to be +0.36 V with respect to a Ag/AgCl reference electrode. A glass ring was then glued and sealed on the chip by silicone to form a small chamber. A photo of the as-fabricated chip was shown in the right panel of Figure S1. Before each electrochemical measurement, the detection chip used was sequentially sonicated in an Alconox solution (8 g Alconox in 1 L water) for 15 min, propan-2-ol for 15 min, and twice in water for 15 min. Electrochemical measurements were performed with an Autolab PGSTAT30 potentiostat/galvanostat (Eco Chemie, The Netherlands) controlled by the General Purpose Electrochemical System (GPES) software (Eco Chemie). DPVs were carried out on the electrode chip using a pulse amplitude of 100 mV/s and a scan rate of 25 mV/s. For each DPV scanning, 50 μL of sample solution was pipetted into the chamber. For the continuous DPV scanning, after adding the sample solution, a paraffin sheet was added to cover and seal the chamber to prevent evaporation of sample solution during measurement.

Native Polyacrylamide Gel Electrophoresis. To prepare the hydrogel, 2.7 mL of 30% acrylamide/bis-acrylamide gel solution (29:1), 1 mL of 10× TAE/Mg^{2+} buffer, 90 μL of 10% ammonium persulfate (APS), 10 μL of *N,N,N′,N′*-tetramethylethylenediamine (TEMED), and 6.2 mL of deionized water were mixed. This mixture contained a final gel percentage of 8%. The gel was polymerized for 1 h at room temperature and then soaked in 1× TAE/Mg^{2+} buffer for use. Five μL of each sample, which was kept in ice after the reaction, was mixed with 1 μL of 6× loading buffer and was subjected to the 8% native polyacrylamide gel electrophoresis (PAGE). The PAGE was performed in ice at a constant voltage of 100 V for 120 min. After staining in 1× SYBR Green I Nucleic Acid Gel Stain solution (Invitrogen, USA) for 20 min, the gels were scanned using a Typhoon TRIO System (GE Medical System, USA). The gel fluorescent images were scanned with excitation/emission wavelengths of 488 nm/520 nm for SybrGreen I and 633 nm/670 nm for Cy5.

AFM Imaging. Assembly products were diluted in 1× TAE/Mg^{2+} buffer and deposited onto freshly cleaved mica (SPI, USA) for 3 min. Samples were then rinsed with deionized water and dried with nitrogen. AFM imaging experiments were performed in air in tapping mode on a Dimension 3100 AFM (Veeco, USA). Silicon probes Tap300Al-G (BudgetSensors, Bulgaria) with resonant frequency 300 kHz, force constant 40 N/m and tip radius 10 nm were used in the experiments. The image background was flattened by Nanoscope IIIa software.

Conflict of Interest: The authors declare no competing financial interest.

Supporting Information Available: Sequences of all strands and supplemental figures. This material is available free of charge *via* the Internet at http://pubs.acs.org.

Acknowledgment. We thank the Research Grants Council of the Hong Kong SAR Government for funding support (RGC 601212).

REFERENCES AND NOTES

1. Drummond, T. G.; Hill, M. G.; Barton, J. K. Electrochemical DNA Sensors. *Nat. Biotechnol.* **2003**, *21*, 1192–1199.
2. Ronkainen, N. J.; Halsall, H. B.; Heineman, W. R. Electrochemical Biosensors. *Chem. Soc. Rev.* **2010**, *39*, 1747–1763.
3. Zhang, H.; Li, F.; Dever, B.; Li, X. F.; Le, X. C. DNA-Mediated Homogeneous Binding Assays for Nucleic Acids and Proteins. *Chem. Rev.* **2013**, *113*, 2812–2841.
4. Fan, C.; Plaxco, K. W.; Heeger, A. J. Electrochemical Interrogation of Conformational Changes as a Reagentless Method for the Sequence-Specific Detection of DNA. *Proc. Natl. Acad. Sci. U.S.A.* **2003**, *100*, 9134–9137.
5. Xiao, Y.; Lou, X. H.; Uzawa, T.; Plakos, K. J. I.; Plaxco, K. W.; Soh, H. T. An Electrochemical Sensor for Single Nucleotide Polymorphism Detection in Serum Based on a Triple-Stem DNA Probe. *J. Am. Chem. Soc.* **2009**, *131*, 15311–15316.

6. Hsieh, K.; White, R. J.; Ferguson, B. S.; Plaxco, K. W.; Xiao, Y.; Soh, H. T. Polarity-Switching Electrochemical Sensor for Specific Detection of Single-Nucleotide Mismatches. *Angew. Chem., Int. Ed.* **2011**, *50*, 11176–11180.
7. Xia, F.; White, R. J.; Zuo, X.; Patterson, A.; Xiao, Y.; Kang, D.; Gong, X.; Plaxco, K. W.; Heeger, A. J. An Electrochemical Supersandwich Assay for Sensitive and Selective DNA Detection in Complex Matrices. *J. Am. Chem. Soc.* **2010**, *132*, 14346–14348.
8. Luo, X.; Lee, T. M. H.; Hsing, I. M. Immobilization-Free Sequence-Specific Electrochemical Detection of DNA Using Ferrocene-Labeled Peptide Nucleic Acid. *Anal. Chem.* **2008**, *80*, 7341–7346.
9. Xuan, F.; Luo, X.; Hsing, I. M. Ultrasensitive Solution-Phase Electrochemical Molecular Beacon-Based DNA Detection with Signal Amplification by Exonuclease III-Assisted Target Recycling. *Anal. Chem.* **2012**, *84*, 5216–5220.
10. Xuan, F.; Luo, X.; Hsing, I. M. Sensitive Immobilization-Free Electrochemical DNA Sensor Based on Isothermal Circular Strand Displacement Polymerization Reaction. *Biosens. Bioelectron.* **2012**, *35*, 230–234.
11. Liu, S.; Lin, Y.; Wang, L.; Liu, T.; Cheng, C.; Wei, W.; Tang, B. Exonuclease III-Aided Autocatalytic DNA Biosensing Platform for Immobilization-Free and Ultrasensitive Electrochemical Detection of Nucleic Acid and Protein. *Anal. Chem.* **2014**, *86*, 4008–4015.
12. Nie, J.; Zhang, D. W.; Zhang, F. T.; Yuan, F.; Zhou, Y. L.; Zhang, X. X. Reporter-Triggered Isothermal Exponential Amplification Strategy in Ultrasensitive Homogeneous Label-Free Electrochemical Nucleic Acid Biosensing. *Chem. Commun.* **2014**, *50*, 6211–6213.
13. Seeman, N. C. DNA in a Material World. *Nature* **2003**, *421*, 427–431.
14. Bath, J.; Turberfield, A. J. DNA Nanomachines. *Nat. Nanotechnol.* **2007**, *2*, 275–284.
15. Zhang, D. Y.; Seelig, G. Dynamic DNA Nanotechnology Using Strand-Displacement Reactions. *Nat. Chem.* **2011**, *3*, 103–113.
16. Pinheiro, A. V.; Han, D.; Shih, W. M.; Yan, H. Challenges and Opportunities for Structural DNA Nanotechnology. *Nat. Nanotechnol.* **2011**, *6*, 763–772.
17. Zhang, D. Y.; Winfree, E. Control of DNA Strand Displacement Kinetics Using Toehold Exchange. *J. Am. Chem. Soc.* **2009**, *131*, 17303–17314.
18. Dirks, R. M.; Pierce, N. A. Triggered Amplification by Hybridization Chain Reaction. *Proc. Natl. Acad. Sci. U.S.A.* **2004**, *101*, 15275–15278.
19. Huang, J.; Wu, Y.; Chen, Y.; Zhu, Z.; Yang, X.; Yang, C. J.; Wang, K.; Tan, W. Pyrene-Excimer Probes Based on the Hybridization Chain Reaction for the Detection of Nucleic Acids in Complex Biological Fluids. *Angew. Chem., Int. Ed.* **2011**, *50*, 401–404.
20. Ren, J.; Wang, J.; Han, L.; Wang, E.; Wang, J. Kinetically Grafting G-Quadruplexes onto DNA Nanostructures for Structure and Function Encoding *via* a DNA Machine. *Chem. Commun.* **2011**, *47*, 10563–10565.
21. Wang, F.; Elbaz, J.; Orbach, R.; Magen, N.; Willner, I. Amplified Analysis of DNA by the Autonomous Assembly of Polymers Consisting of DNAzyme Wires. *J. Am. Chem. Soc.* **2011**, *133*, 17149–17151.
22. Shimron, S.; Wang, F.; Orbach, R.; Willner, I. Amplified Detection of DNA through the Enzyme-Free Autonomous Assembly of Hemin/G-Quadruplex DNAzyme Nanowires. *Anal. Chem.* **2012**, *84*, 1042–1048.
23. Chen, Y.; Xu, J.; Su, J.; Xiang, Y.; Yuan, R.; Chai, Y. *In Situ* Hybridization Chain Reaction Amplification for Universal and Highly Sensitive Electrochemiluminescent Detection of DNA. *Anal. Chem.* **2012**, *84*, 7750–7755.
24. Xu, Q.; Zhu, G.; Zhang, C. Homogeneous Bioluminescence Detection of Biomolecules Using Target-Triggered Hybridization Chain Reaction-Mediated Ligation without Luciferase Label. *Anal. Chem.* **2013**, *85*, 6915–6921.
25. Ge, Z.; Lin, M.; Wang, P.; Pei, H.; Yan, J.; Shi, J.; Huang, Q.; He, D.; Fan, C.; Zuo, X. Hybridization Chain Reaction Amplification of MicroRNA Detection with a Tetrahedral DNA Nanostructure-Based Electrochemical Biosensor. *Anal. Chem.* **2014**, *86*, 2124–2130.
26. Yin, P.; Choi, H. M. T.; Calvert, C. R.; Pierce, N. A. Programming Biomolecular Self-Assembly Pathways. *Nature* **2008**, *451*, 318–322.
27. Chandran, H.; Rangnekar, A.; Shetty, G.; Schultes, E. A.; Reif, J. H.; LaBean, T. H. An Autonomously Self-Assembling Dendritic DNA Nanostructure for Target DNA Detection. *Biotechnol. J.* **2013**, *8*, 221–227.
28. Xuan, F.; Hsing, I. M. Triggering Hairpin-Free Chain-Branching Growth of Fluorescent DNA Dendrimers for Nonlinear Hybridization Chain Reaction. *J. Am. Chem. Soc.* **2014**, *136*, 9810–9813.
29. Egholm, M.; Buchardt, O.; Christensen, L.; Behrens, C.; Freier, S. M.; Driver, D. A.; Berg, R. H.; Kim, S. K.; Norden, B.; Nielsen, P. E. PNA Hybridizes to Complementary Oligonucleotides Obeying the Watson–Crick Hydrogen-Bonding Rules. *Nature* **1993**, *365*, 566–568.
30. Li, S. J.; Li, J.; Wang, K.; Wang, C.; Xu, J. J.; Chen, H. Y.; Xia, X. H.; Huo, Q. A Nanochannel Array-Based Electrochemical Device for Quantitative Label-free DNA Analysis. *ACS Nano* **2010**, *4*, 6417–6424.
31. Seelig, G.; Soloveichik, D.; Zhang, D. Y.; Winfree, E. Enzyme-Free Nucleic Acid Logic Circuits. *Science* **2006**, *314*, 1585–1588.
32. Zhang, D. Y.; Chen, S. X.; Yin, P. Optimizing the Specificity of Nucleic Acid Hybridization. *Nat. Chem.* **2012**, *4*, 208–214.
33. Zadeh, J. N.; Steenberg, C. D.; Bois, J. S.; Wolfe, B. R.; Pierce, M. B.; Khan, A. R.; Dirks, R. M.; Pierce, N. A. NUPACK: Analysis and Design of Nucleic Acid Systems. *J. Comput. Chem.* **2011**, *32*, 170–173.
34. Gao, Y.; Wolf, L. K.; Georgiadis, R. M. Secondary Structure Effects on DNA Hybridization Kinetics: A Solution *versus* Surface Comparison. *Nucleic Acids Res.* **2006**, *34*, 3370–3377.